OPEN

Semiconductor nanoparticle-based hydrogels prepared via self-initiated polymerization under sunlight, even visible light

Da Zhang[1]*, Jinhu Yang[1,4]*, Song Bao[1], Qingsheng Wu[1,2] & Qigang Wang[1,2,3]

[1]Department of Chemistry, Tongji University, Siping Road 1239, Shanghai 200092, P. R. China, [2]Key Laboratory of Yangtze River Water Environment, Ministry of Education, Siping Road 1239, Shanghai 200092, PR China, [3]Advanced Research Institute, Tongji University, Siping Road 1239, Shanghai 200092, P. R. China, [4]Institute for Biomedical Engineering & Nano Science, Tongji University, Siping Road 1239, Shanghai 200092, P. R. China.

Since ancient times, people have used photosynthesized wood, bamboo, and cotton as building and clothing materials. The advantages of photo polymerization include the mild and easy process. However, the direct use of available sunlight for the preparation of materials is still a challenge due to its rather dilute intensity. Here, we show that semiconductor nanoparticles can be used for initiating monomer polymerization under sunlight and for cross-linking to form nanocomposite hydrogels with the aid of clay nanosheets. Hydrogels are an emerging multifunctional platform because they can be easily prepared using solar energy, retain semiconductor nanoparticle properties after immobilization, exhibit excellent mechanical strength (maximum compressive strength of 4.153 MPa and tensile strength 1.535 MPa) and high elasticity (maximum elongation of 2784%), and enable recyclable photodegradation of pollutants. This work suggests that functional nanoparticles can be immobilized in hydrogels for their collective application after combining their mechanical and physiochemical properties.

Hydrogels, which have a three-dimensional porous network, have attracted significant attention due to their use as biomaterials and model matrices for biological studies[1–3]. Most hydrogels, whether covalently or non-covalently cross-linked, are mechanically weak and exhibit poor elasticity and a lack of physiochemical functions[4]. Pioneering double network hydrogels can achieve certain mechanical requirements using a typical two-step polymerization[5,6]. A nanocomposite (NC) hydrogel is another original material that can achieve ultra-high mechanical properties due to the multiple non-covalent effects between clay nanosheets (Clay-NS) and polyacrylamide chains[7–10]. Recently, researchers have developed a supramolecular hydrogel by mixing Clay-NS with dendritic polymers using a multiple salt bridge[11]. However, the preparation of these tough hydrogels requires complicated molecular designs or preparation processes and does not permit the combination of the strengths and functions of the individual components. Until now, semiconductor nanoparticles (NPs) could only be immobilized in weak polymer hydrogels by physical mixing or by vinyl-modified covalent cross-linking[12–14].

Here, we chose a sunlight-initiated approach to prepare multifunctional NC hydrogels using semiconductor NPs as the initiator and backbone; this approach combines the mechanical properties and physiochemical performances of the materials into a single platform. Our system consists of four components: water, water-soluble semiconductor nanoparticles (ZnO, TiO_2, Fe_2O_3, SnO_2, ZrO_2, CdSe, or CdTe), N,N-dimethylacrylamide (DMAA), and Clay-NS. Semiconductor NPs, including TiO_2, ZnO, and CdTe, have been shown to undergo photo-initiated polymerization during heterogeneous polymer synthesis[15–18]. These inorganic initiators have rarely been used to prepare polymer gels under light. The DMAA monomer is a water-soluble acrylamide derivative, and the corresponding PDMAA exhibits stability against hydrolytic effects and temperature changes. We recently observed that sunlight irradiation can increase the viscosity of a mixture of semiconductor NPs and DMAA due to polymerization. The insufficient number of cross-linking points on the NP surfaces determine the final viscous situation other than three-dimensional hydrogel. This phenomenon suggests the possibility of preparing semiconductor NP-based hydrogels under sunlight by introducing additional cross-linking points. Based on the literature, we introduced Clay-NS, a layered structured mineral with a high specific surface[19], to the mixture as a second building block.

Results

Preparation and characterization. A dispersion of semiconductor NPs, DMAA, and Clay-NS (Figure 1a) was used as a precursor. Of these materials, the semiconductor NPs can initiate the polymerization under sunlight to form inorganic-PDMAA brushes (Figure 1b) and a non-covalent NC hydrogel network via the further cross-linking of the brushes (Figure 1c)[7,8,20,21]. As described in the Methods section, a typical ZnO nanoparticle-based nanocomposite hydrogel (ZnO-NC gel) was prepared from an aqueous solution (Figure 1d) with 0.2% ZnO, 5.0% DMAA, and 5.0% Clay-NS (Supplementary movie). The final ZnO-NC gel was translucent and tough after approximately 1 h of sunlight irradiation (Figures 1e and 1f and Supplementary Figure S1). As shown in Table 1 and in Supplementary Figure S2, simple sunlight irradiation yielded elastic and functional NC hydrogels with various nanoparticles, with the exception of ZrO_2 and Fe_2O_3 nanoparticles. We used a xenon lamp with an AM 1.5 G filter to mimic sunlight (similar spectrum composition and equivalent intensity). All functional nanoparticles, with the exception of ZrO_2 and Fe_2O_3, can be used in similar preparations under artificial sunlight. For quantum dots (CdSe and CdTe) with a low bandgap, an elastic hydrogel was prepared via visible light irradiation with a wavelength over 420 nm (Supplementary Figure S3), which can be produced by cutting off the UV light of artificial sunlight. A morphology analysis confirms the fabrication of a functional NC hydrogel using three components. SEM analysis of a supercritically treated sample (Figure 1g) reveals irregular pores with sizes ranging from several tens to several hundreds of nanometres and highly dispersed brushes 100–300 nm in size. The porous aerogel was tough rather than fragile, in contrast to traditional inorganic aerogels. Bio-cutting TEM analysis (Figure 1h) reveals that aggregated NPs, with sizes of approximately several tens of nanometres, and individual Clay-NS particles, which have the same size as in solution, were dispersed in the gel (Supplementary Figure S4).

In our functional hydrogels, the photoinitiator semiconductor NPs were similar to organic initiators[20,21], which enable spatial/temporal control and a mild curing process relative to the traditional preparation of most hydrogels[22–34]. The important advantages of this method include the use of inexhaustible sunlight as a substitute for an ultraviolet generator. The mild light irradiation initiated by successful semiconductor NPs can lead to the effective and complete polymerizations of DMAA. Other acrylamide derivatives, such as N-isopropylacrylamide, can also be polymerized via the irradiation effect. Time-dependent ^{1}H NMR analysis of the TiO_2 precursors exhibits an approximately 99% DMAA conversion rate after 1 h of irradiation under sunlight and under artificial light (Figure 2a and Supplementary Figures S5 and S6). The clear gelation of these precursors during irradiation occurs concurrently with a rapid increase
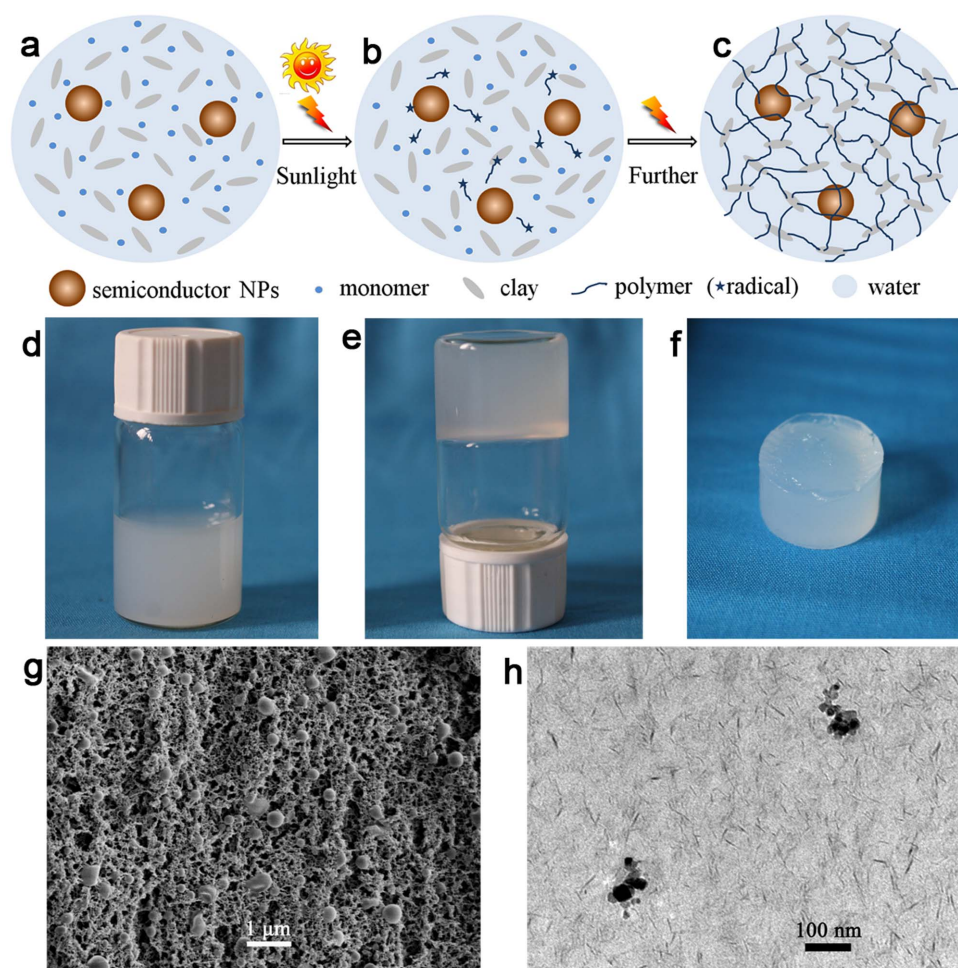

Figure 1 | Proposed mechanism, photographs, and SEM and TEM images of the functional ZnO-NC hydrogel. (a–c) Proposed mechanism of the functional NC hydrogels under sunlight. The semiconductor NPs, monomer, and Clay-NS are homogeneously dispersed in water (a). When exposed to sunlight, polymerization is initiated by the semiconductor NPs (b). Next, the NPs and Clay-NS are cross-linked to develop a 3D network (c). (d–f) Optical images of the hydrogelation process. A mixture solution of ZnO nanoparticles, DMAA, and Clay-NS (d). Hydrogelation after 1 h of irradiation (e). The elastic ZnO-NC hydrogel (f). (g) SEM image of the ZnO-NC hydrogel after supercritical drying. (h) TEM image of the ZnO-NC hydrogel after a bio-cutting treatment.

Table 1 | The gelation ability of various semiconductor nanoparticles

NP	Absorption edge (nm)	Band energy (eV)	Solution colour	Sun light[a]	Xenon lamp[a]	Visible light[b]
Fe_2O_3	919.1	1.35	Red brown	No	No	No
CdSe	570.4	2.17	Yellow	Gel	Gel	Gel
CdTe	559.8	2.22	Yellow	Gel	Gel	Gel
ZnO	434.2	2.85	Translucent	Gel	Gel	No
TiO_2	414.8	2.99	White	Gel	Gel	No
SnO_2	384.9	3.22	Translucent	Gel	Gel	No
ZrO_2	250.3	4.95	White	No	No	No

[a]The average intensities of sunlight and of the xenon lamp with an AM 1.5 G filter at 365 nm are both approximately 2.0 mw cm^{-2}.
[b]The visible region of the xenon lamp was obtained by cutting off the light at $\lambda < 420$ nm.

in monomer conversion after 15 min (Figure 2a), which accompanies by a sharp increase in the decay time and a decrease in the correlation coefficient and the dynamic light scattering (DLS) spectrum (Figure 2b). Comparison of the small angle X-ray scattering (SAXS) spectra at various irradiation times reveals the formation of a regular pore structure (Supplementary Figure S7). If a light source with a higher intensity is used, the gelation could be completed more rapidly; this phenomenon was investigated using an *in situ* rheological measurement with strong ultraviolet light (Supplementary Figure S8). For a visible light-irradiated CdTe system, a greater than 95% DMAA conversion rate can be achieved within 1.5 h (Supplementary Figure S9). Other semiconductor NPs, such as ZnO, SnO_2, CdS, and CdSe, also permit polymerization irradiation under various light sources. For the exceptions, the ZrO_2 and Fe_2O_3 nanoparticles, the NMR data indicate a <5% DMAA conversion rate after the same irradiation time (Supplementary Figure S10). The large bandgap of ZrO_2 (4.95 eV) is most likely the main barrier to

electron-hole excitation. Although Fe_2O_3 nanoparticles can initiate photo-polymerization in organic solvents, the free radicals are easily inhibited by the reduction of Fe^{3+} and water molecules in an aqueous solution[18]. For use in our self-initiated system, a semiconductor NP should have a moderate bandgap, which is easy to be excited by sunlight to form active radicals.

Mechanical properties. As shown in the supporting movie, our semiconductor NP-NC gels exhibits high toughness and elasticity. Table 2 lists the detailed mechanical data for the TiO_2-NC hydrogels with various semiconductor NP and Clay-NS proportions. A three-component hydrogel could be formed with a proper concentration range of NPs (0.015% to 1% for TiO_2, ZnO, SnO_2, CdSe, and CdTe), DMAA (5% to 10%), and Clay-NS (5% to 20%). As shown in Figure 3a, the TiO_2-NC hydrogels with 0.2% TiO_2 (5% DMAA and 5% Clay-NS) exhibit a very large elongation of close to 27 times the original length. The minimum proportion of TiO_2 for complete
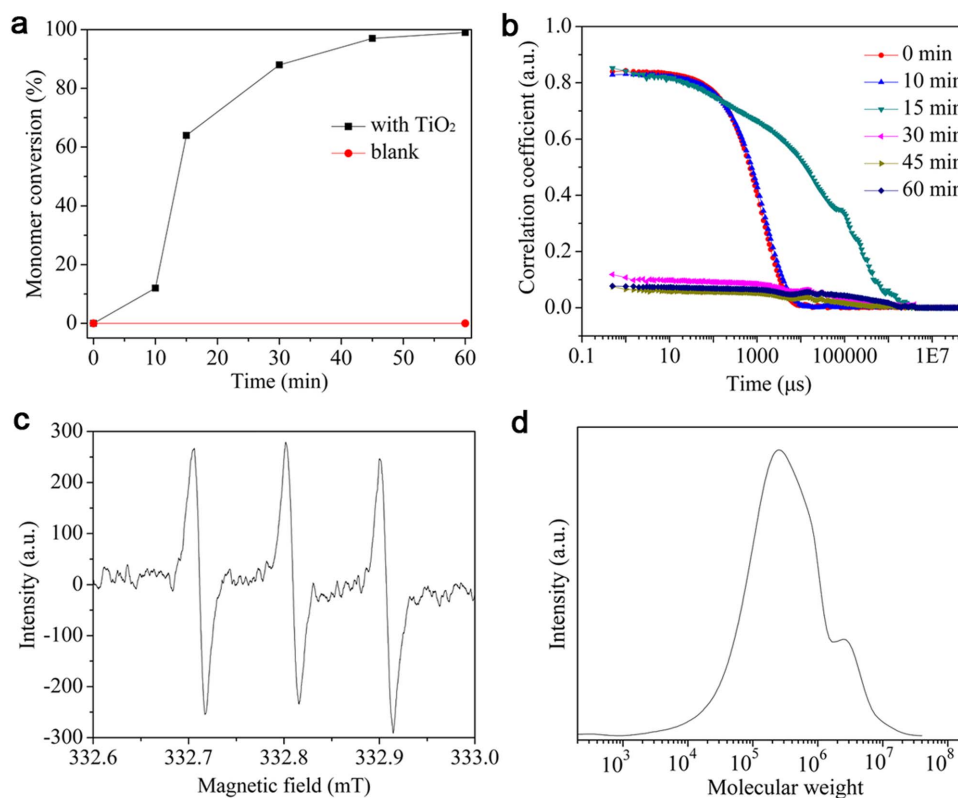

Figure 2 | Gelation process of the TiO_2-NC hydrogels. (a) The conversion of the monomer by TiO_2 under a xenon lamp with an AM 1.5 G filter. The precursor consisted of 3% DMAA, 3% Clay-NS, 94% D_2O, and 0.1% TiO_2. (b) DLS analysis of the sample during irradiation. The precursor solution containing 3% DMAA, 3% clay, 94% H_2O, and 0.1% TiO_2 was irradiated for different times. (c) The EPR spectrum of the precursor consisting of TiO_2 and DMAA under UV irradiation. (d) The molecular weight distribution of the PDMAA polymers formed from the aqueous mixture of TiO_2 and DMAA after 1 h of sunlight irradiation.

Table 2 | The mechanical properties of the TiO₂-NC gels with various proportions

No.	Composition TiO2/ DMAA/Clay-NS (%)	Tensile Modulus (MPa)	Tensile Strength (MPa)	Exten-sibility (%)	Comp.ᵃ Modulus (MPa)	Comp.ᵃ Strength (MPa)ᵇ
1	0.2/5/5	0.0082 ± 0.0004	0.2575 ± 0.0143	2688 ± 73	0.0074 ± 0.0004	0.386 ± 0.011
2	0.2/7/5	0.0081 ± 0.0004	0.2525 ± 0.0125	2784 ± 58	0.0068 ± 0.0004	0.363 ± 0.009
3	0.2/10/5	0.0083 ± 0.0003	0.2595 ± 0.0108	2767 ± 80	0.0063 ± 0.0004	0.335 ± 0.008
4	0.2/10/10	0.167 ± 0.026	1.130 ± 0.074	2280 ± 103	0.177 ± 0.011	2.103 ± 0.116
5	0.2/10/15	0.507 ± 0.032	1.535 ± 0.089	1506 ± 78	0.610 ± 0.026	3.356 ± 0.143
6	0.2/10/20	2.404 ± 0.150	1.075 ± 0.063	1086 ± 86	1.958 ± 0.080	4.153 ± 0.121

ᵃComp. = Compressive.
ᵇCompressive strength at a maximum strain of 95%.

conversion is 0.05%, which yields an approximate elongation of 2740%. Figure 3b shows that the relative elongation decreases slightly to 2720%, 2688%, and 2608% when the proportion of TiO_2 increases to 0.1%, 0.2%, and 0.4%, respectively. The additional cross-linking density from TiO_2 nanoparticles should correspond to a decrease in the elongation of our hydrogels along with an increase in the proportion of TiO_2. As shown in Supplementary Figure S12, the ZnO-based hydrogel also exhibits decreasing elongation as the proportion of ZnO was increased. The final optimized concentration of TiO_2 in our system is 0.2%, taking into account the elongation, tensile modulus, and broken strength (Figure 3b). Synthetic PDMAA with a broad distribution provides the high elasticity of our NC gel system, which is the result of the space linkage between the dispersed inorganic cross-linkers.

The tensile performances (elongation, modulus, and strength) all weakly depend on the DMAA content when the concentration is greater than 5%. A maximum elongation of 2784% occurs for the TiO_2-NC gel containing 7% DMAA (0.2% TiO_2 and 5% Clay-NS). We select 5% DMAA as the optimized concentration to decrease the organic component and the final cost. The tensile performance (elongation, modulus, and strength) all strongly depend on the Clay-NS content (Figure 3c and Table 2). Therefore, we attempt to use the viscous precursors to fabricate a hydrogel with up to 20% Clay-NS, which should have excellent mechanical properties due to the high inorganic concentration. The maximum tensile modulus of the functional NC gel with 20% Clay-NS (0.2% TiO_2 and 10% DMAA) is 2.404 MPa. The elongation values decrease from 2688% to 1086% as the proportion of Clay-NS increase from 5–20% due to the increased cross-linking density. A maximum broken strength of 1.535 MPa is obtained for the functional NC gel with 15% Clay-NS.

For the compressive test, we found that all of the hydrogels can tolerate a compression greater than 95% and can exhibit partially rubber-like properties. The compressive performances of the hydrogels decrease slightly with increasing DMAA concentration (0.2% TiO_2 and 5% Clay-NS) (Table 2). The compressive modulus and strength both strongly depend on the Clay-NS content. As shown in Figure 3d, the compressive modulus and strength at a 95% strain increase with increasing Clay-NS amount. The TiO_2-NC hydrogel
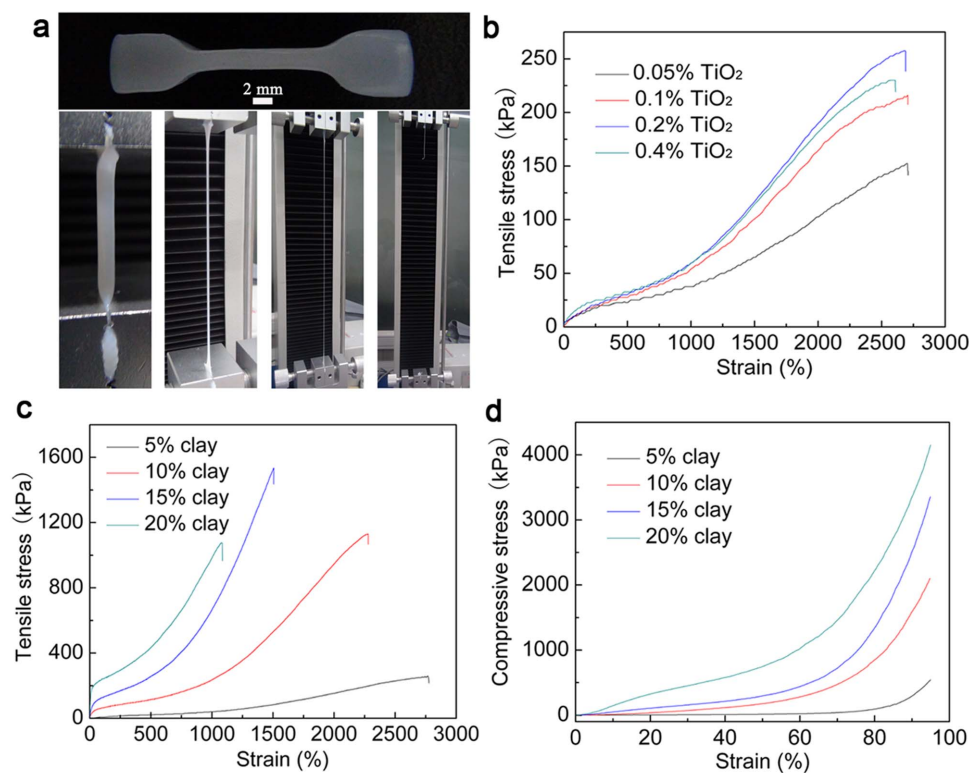

Figure 3 | Mechanical properties of the TiO₂-NC hydrogels with different proportions. (a) Images of the TiO_2-NC hydrogel during the tensile testing process. (b) Tensile properties of the TiO_2-NC hydrogels containing 5% DMAA, 5% clay, and different proportions of TiO_2. (c) Tensile properties of the TiO_2-NC hydrogels containing 0.2% TiO_2 and different Clay-NS concentrations. (d) Compressive properties of the TiO_2-NC hydrogels with different clay concentrations.

(0.2% TiO_2, 5% DMAA, and 20% Clay-NS) achieves a maximum of 1.958 MPa for the compressive modulus and 4.153 MPa for the compressive strength. Other semiconductor NP-NC gels, such as the ZnO system, also exhibited excellent compressive performances similar to that of the TiO_2 gels (Supplementary Figures S11 and S12). Another interesting mechanical property is the very rapid recovery of rheological strength that our sample exhibits after a large-amplitude oscillatory breakdown; this property is known as self-healing[35,36] (Supplementary Figure S13). This recovery is fully reproducible for three strain cycles (γ changes as 1%-100%-1%-100%-1%-100%-1%).

Fluorescence and photocatalytic properties. One advantage of our systems is the remnant physicochemical properties of the semiconductor NPs after *in situ* immobilization. We can observe that the NPs within a tough hydrogel retain their intrinsic properties. As shown in Figure 4a, the CdTe-NC hydrogel (CdTe/DMAA/Clay-NS of 0.015%/3%/3%) has absorption and emission peaks that are analogous to those of a 0.015% quantum dot solution of CdTe. The fluorescence intensity of the CdTe-NC hydrogel is slightly higher than that of the original CdTe solution at an identical concentration due to light activation during processing[37]. Hydrogels with different fluorescence intensities can be easily prepared using variously sized CdTe dots (Figures 4b–d).

Semiconductor NPs can act as photocatalysts even within a functional hydrogel. The TiO_2-NC hydrogel (TiO_2/DMAA/Clay-NS of 0.4%/5%/5%) is selected to collectively treat dyes using the adsorption-photodegradation-readsorption cycle[38,39]. As drawn in Figure 4e, the TiO_2-NC hydrogel can enrich a large amount of methylene blue to form a dark blue hydrogel via the electrostatic effect. The first maximum absorption of methylene blue is 59.5 mg for 1 g of dried hydrogel (Figure 4f). The dark blue hydrogel in 5-fold excess of water can change to light blue after 2 h of UV (middle-pressure mercury lamp, 100 mW cm^{-2}) degradation via the loaded TiO_2. The colourless products after photodegradation easily diffuse in water. Notably, the reused TiO_2-NC hydrogel can readsorb the methylene blue and be re-treated by the immobilized photocatalyst. The adsorbed amount of methylene blue after two recycles can reach 86.3% of the fresh hydrogel. As a control, the traditional NC hydrogel of Clay-NS and DMAA[8] was studied; this hydrogel could adsorb an equivalent amount of methylene blue but could not be obviously degraded under the same UV irradiation conditions (Supplementary Figure S14). Another pollutant, acid fuchsin can also be captured and degraded with the TiO_2-NC hydrogel (Supplementary Figure S15).

Discussion

With our aqueous precursors, semiconductor NPs produce the same free radical mechanism as organic initiators[20,21] due to water inhibition of the chain propagated ions. The OH radical (produced by the photogenerated hole and electron) and the hole are the two initiating species that form a DMAA radical and further propagating radicals. The competitive OH radical is the main species in our precursor with a high pH (approximately 9.0) in the absence of deliberate degassing treatment[15]. The existence of a hydroxyl radical in the TiO_2 and CdTe base solutions is confirmed by electron paramagnetic resonance (EPR) spectroscopy after DMPO adduction; the spectroscopy data reveal a characteristic DMPO-OH radical spectrum with a 1:2:2:1
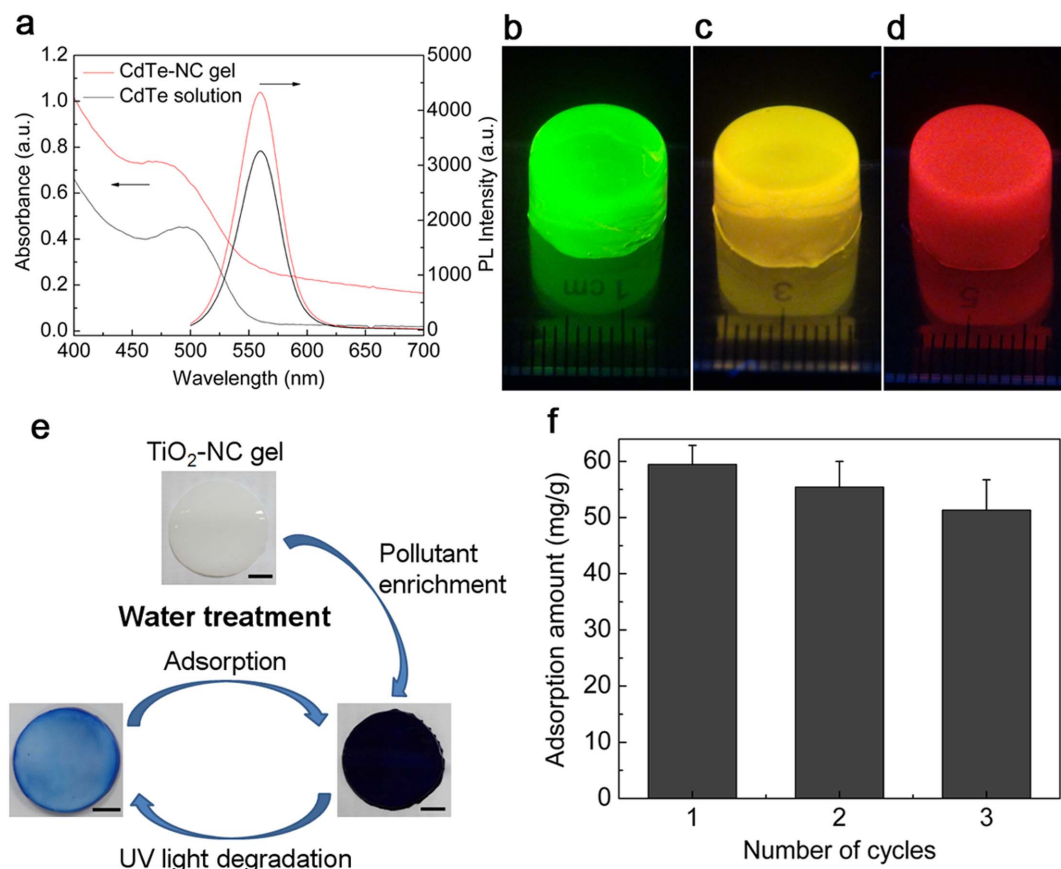

Figure 4 | Fluorescence and photocatalytic properties of the semiconductor NP-NC hydrogels. (a) The UV-Vis absorbance and PL spectra of the CdTe-NC hydrogel and the CdTe quantum dot solution with the same concentration of CdTe. (b–d) Images of three different CdTe-NC hydrogels under an ultraviolet lamp. The average diameters of the CdTe quantum dots are estimated to be 2.8 nm (b, green), 3.3 nm (c, yellow), and 4.0 nm (d, red). (e) The recyclable application of the TiO_2-NC hydrogel for the treatment of polluted water and images of the TiO_2-NC hydrogels at various stages are shown (the scale is 1 cm). (f) The amount of MB adsorbed by the TiO_2-NC gel in the three reusing cycles.

ratio (Supplementary Figures S16a and 16c). The hole initiator can directly react with non-covalent adsorbed DMAA to form a surface monomer radical by abstracting hydrogen, while the active OH radical can also adduct with DMAA to form a monomer radical[15–18]. The long-lived propagating radical that grows from the monomer radical is obvious in the EPR spectrum of the mixture solution of TiO₂ and DMAA after UV irradiation (Figure 2c) and in the spectrum of the CdTe solution system (Supplementary Figure S16d) after visible light irradiation.

The formation of PDMAA polymers with a broad molecular weight distribution after 1 h of sunlight irradiation is confirmed by the GPC data for the mixture solution of TiO₂ and DMAA (Figure 2d). The propagating radical signal has the largest intensity at 4 min and then decreases with time (Supplementary Figure S16b). The semiconductor NPs should be immobilized within the functional hydrogels because the non-covalent cross-linking points prevent easy leakage during incubation. A mechanism for the preparation of our NC gels under sunlight irradiation is proposed as follows. First, more active holes react with the non-covalent adsorbed DMAA to form a surface monomer radical, which initiates the polymerization directly at the unmovable NP surfaces. The corresponding polymers exhibit both double bond and hydroxyl end groups (Supplementary Figure S17a). The OH radicals then diffuse from the NPs and initiate polymerization near the NP surfaces in the polymers that only have hydroxyl end groups (Supplementary Figure S17b).

Our semiconductor NP-based NC gels, which are produced by easy sunlight-initiated polymerization and a non-covalent cross-linking effect, have not only mechanical properties that are tuneable by changing the various components but also no toxic residue in comparison with organic initiators. The self-immobilized NPs within the functional NC gels exhibit inherent physiochemical properties, such as absorption and fluorescence, that are comparable to those of their original solution. The semiconductor NP-NC hydrogels can be used as a recyclable platform for the collective treatment of industrial pollutants. By coupling other applications of NPs, functional NC gels could be designed as an effective and recyclable water-rich platform for photohydrolysis and solar cells. Our semiconductor NP-based hydrogel addresses one disadvantage of hydrogels fabricated by complicated methods, that is, excellent mechanical performances but a lack of functionality.

Methods

Preparation. In a typical hydrogelation, 0.12 mL of a ZnO aqueous suspension (10%), DMAA monomer (300 mg, 0.31 mL), Clay-NS (300 mg), and water were mixed with vigorous stirring to form a 6.0 g aqueous suspension within 5 minutes (Figure 1d). The last precursor can form a ZnO-NC gel with semitransparent performance and tough elasticity via irradiation under sunlight (1 h, average intensity of 2.0 mW cm⁻² at 365 nm) or artificial sunlight (1 h, fixed intensity of 2.0 mW cm⁻² at 365 nm provided by a xenon lamp with an AM 1.5 G filter, Model 91160, 300 W, Newport, USA, Full Spectrum Solar Simulator) (Figure 1e). The other semiconductor NPs can be used for a similar preparation with artificial sunlight or even visible light based on their different bandgaps.

Characterizations. We used NMR to demonstrate the conversion of the monomer in D₂O using 1,4-dioxane as the internal standard material. The molecular structures of the resulting polymer products were also analyzed by NMR. Compressive stress-strain measurements were performed on gels with a tensile-compressive tester (FR-108B, Farui Co.). A cylindrical gel sample 13 mm in diameter and 7 mm thick was set on the lower plate and compressed by the upper plate, which was connected to a load cell (500 N), at a strain rate of 5 mm min⁻¹. Tensile measurements were acquired using a hydrogel sample with a dumbbell shape (20 mm × 2 mm × 2 mm). SEM images of a supercritically treated sample were acquired on a Hitachi S-4800 scanning electron microscope (SEM). TEM pictures of bio-cutting samples were acquired on a JEM-2010 transmission electron microscopy (TEM) at a 120 kV accelerating voltage. The molecular weights of the polymers were determined from Gel Permeation Chromatography measurements (Waters 2695, GPC). DLS analysis of the gelation process was performed on a Zetasizer instrument (Nano-ZS, Malvern). EPR analysis of the free radicals was conducted with an EPR Spectrometer (A300, Bruker). The SAXS measurements of the gelation process were acquired at the Shanghai Synchrotron Radiation Facility, Shanghai, China, at the small angle X-ray scattering station (BL16B1) with a long-slit collimation system. UV-Vis spectra and

photoluminescence (PL) spectra were obtained on a UV-Vis spectrometer (Agilent 8453) and a fluorescence spectrometer (Hitachi F-7000), respectively.

1. Wang, H., Yang, Z. & Adams, D. J. Controlling peptidebased hydrogelation. *Mater. Today* **15**, 500–507 (2012).
2. Yan, B., Boyer, J. C., Habault, D., Branda, N. R. & Zhao, Y. Near Infrared Light Triggered Release of Biomacromolecules from Hydrogels Loaded with Upconversion Nanoparticles. *J. Am. Chem. Soc.* **134**, 16558–16561(2012).
3. Kouwer, P. H. J. *et al*. Responsive biomimetic networks from polyisocyanopeptide hydrogels. *Nature* doi:10.1038/nature11839 (2013).
4. Peppas, N. A., Huang, Y., Torres-Lugo, M., Ward, J. H. & Zhang, J. Physicochemical, foundations and structural design of hydrogels in medicine and biology. *Annu. Rev. Biomed. Eng.* **2**, 9–29 (2000).
5. Gong, J. P., Katsuyama, Y., Kurokawa, T. & Osada, Y. Double-network hydrogels with extremely high mechanical strength. *Adv. Mater.* **15**, 1155–1158 (2003).
6. Chen, Y. M., Yang, J. J., Osada, Y. & Gong, J. P. Synthetic hydrogels as scaffolds for manipulating endothelium cell behaviors. *Chin. J. Polym. Sci.* **29**, 23–41 (2011).
7. Haraguchi, K. & Takehisa, T. Nanocomposite hydrogel: a unique organic-inorganic network structure with extraordinary mechanical, optical, and swelling/de-swelling properties. *Adv. Mater.* **14**, 1120–1124 (2002).
8. Haraguchi, K., Farnworth, R., Ohbayashi, A. & Takehisa, T. Compositional effects on mechanical properties of nanocomposite hydrogels composed of poly(N, N-dimethylacrylamide) and clay. *Macromolecules* **36**, 5732–5741 (2003).
9. Liu, Y., Zhu, M. F., Liu, X. L., Zhang, W. & Adler, H. J. P. High clay content nanocomposite hydrogels with surprising mechanical strength and interesting deswelling kinetics. *Polymer* **47**, 1–5 (2006).
10. Wang, J. F., Lin, L., Cheng, Q. F. & Jiang, L. A strong bio-inspired layered pnipam-clay nanocomposite hydrogel. *Angew. Chem. In. Ed.* **51**, 4676–4680 (2012).
11. Wang, Q. G., Mynar, J. L., Yoshida, M., Lee, E., Lee, M. & Aida, T. High-water-content mouldable hydrogels by mixing clay and a dendritic molecular binder. *Nature* **463**, 339–343 (2010).
12. Satarkar, N. S., Biswal, D. & Hilt, J. Z. Hydrogel nanocomposites: a review of applications as remote controlled biomaterials. *Soft Matter* **6**, 2364–2371 (2010).
13. Wang, C., Flynn, N. T. & Langer, R. Controlled structure and properties of thermoresponsive nanoparticle–hydrogel composites. *Adv. Mater.* **16**, 1074–1079 (2004).
14. Zhu, C. H., Hai, Z. B., Cui, C. H., Li, H. H. & Yu, S. H. In situ controlled synthesis of thermosensitive poly(N-isopropylacrylamide)/Au nanocomposite hydrogels by gamma radiation for catalytic application. *Small* **8**, 930–936 (2012).
15. Ni, X. Y., Ye, J. & Dong, C. Kinetics studies of methyl methacrylate photopolymerization initiated by titanium dioxide semiconductor nanoparticles. *J. Photoch. Photobio. A* **181**, 19–27 (2006).
16. Huang, Z. Y., Barber, T., Mills, G. & Morris, M. B. Heterogeneous photopolymerization of methyl-methacrylate initiated by small ZnO particles. *J. Phys. Chem.* **98**, 12746–12752 (1994).
17. Nakashima, T., Sakashita, M., Nonoguchi, Y. & Kawai, T. Sensitized photopolymerization of an ionic liquid-based monomer by using CdTe nanocrystals. *Macromolecules* **40**, 6540–6544 (2007).
18. Stroyuk, A. L. *et al*. Photoinitiation of butylmethacrylate polymerization by colloidal semiconductor nanoparticles. *J. Photoch. Photobio. A* **162**, 339–351 (2004).
19. Rockwood Additives Ltd., Laponite in personal care products. *Laponite technical bulletin* L211/01g (1990).
20. Ferse, B. *et al*. Gelation mechanism of poly(N-isopropylacrylamide)-clay nanocomposite hydrogels synthesized by photopolymerization. *Langmuir* **24**, 12627–12635 (2008).
21. Haraguchi, K. & Takada, T. Synthesis and characteristics of nanocomposite gels prepared by in situ photopolymerization in an aqueous system. *Macromolecules* **43**, 4294–4299 (2010).
22. Hirst, A. R., Escuder, B., Miravet, J. F. & Smith, D. K. High-tech applications of self-assembling supramolecular nanostructured gel-phase materials: from regenerative medicine to electronic devices. *Angew. Chem. Int. Ed.* **47**, 8002–8018 (2008).
23. Zhang, X. L. *et al*. Rational Design of a Tetrameric Protein to Enhance Interactions between Self-Assembled Fibers Gives Molecular Hydrogels. *Angew. Chem. Int. Ed.* **51**, 4388–4392 (2012).
24. Kiyonaka, S. *et al*. Semi-wet peptide/protein array using supramolecular hydrogel. *Nature Mater.* **3**, 58–64 (2004).
25. Gao, Y., Zhao, F., Wang, Q. G., Zhang, Y. & Xu, B. Small peptide nanofibers as the matrices of molecular hydrogels for mimicking enzymes and enhancing the activity of enzymes. *Chem. Soc. Rev.* **39**, 3425–3433 (2010).
26. Ladet, S., David, L. & Domard, A. Multi-membrane hydrogels. *Nature* **452**, 76–79 (2008).
27. Liang, G. L., Ren, H. J. & Rao, J. H. A biocompatible condensation reaction for controlled assembly of nanostructures in living cells. *Nature Chem.* **2**, 54–60 (2010).
28. Sun, J. Y., Zhao, X. H., Mooney, D. J., Vlassak, J. J. & Suo, Z. G. Highly stretchable and tough hydrogels. *Nature* **489**, 133–136 (2012).
29. John, G., Jadhav, S. R., Menon, V. M. & John, V. T. Flexible Optics: Recent Developments in Molecular Gels. *Angew. Chem. Int. Ed.* **8**, 1760–1762 (2012).

30. Carretti, E., Dei, L. & Weiss, R. G. Soft matter and art conservation. Rheoreversible gels and beyond. *Soft Matter* **1**, 17–22 (2005).
31. Adams, D. J. *et al.* A new method for maintaining homogeneity during liquid-hydrogel transitions using low molecular weight hydrogelators. *Soft Matter* **5**, 1856–1862 (2009).
32. Banwell, E. F., Adelardo, E. S., Adams, D. J., Butler, M. F. & Woolfson, D. N. Rational design and application of responsive alpha-helical peptide hydrogels. *Nature Mater.* **8**, 596–600 (2009).
33. Hirst, A. R., Smith, D. K., Feiters, M. C., Geurts, H. P. M. & Wright, A. C. Two-component dendritic gels: easily tunable materials. *J. Am. Chem. Soc.* **125**, 9010–9011 (2003).
34. Ke, J. H., Wang, Z. K., Li, Y. Z., Hu, Q. L. & Feng, J. Ferroferric oxide/chitosan scaffolds with three-dimensional oriented structure. *Chin. J. Polym. Sci.* **30**, 436–442 (2012).
35. Yoshida, M. *et al.* Oligomeric electrolyte as a multifunctional gelator. *J. Am. Chem. Soc.* **129**, 11039–11041 (2007).
36. Nowak, A. P. *et al.* Rapid recovering hydrogel scaffolds from self-assembling diblock copolypeptide amphiphiles. *Nature* **417**, 424–428 (2002).
37. Li, J. *et al.* Highly photoluminescent CdTe/Poly(N-isopropylacrylamide) temperature -sensitive gels. *Adv. Mater.* **17**, 163–166 (2005).
38. Hoffmann, M. R., Martin, S. T., Choi, W. Y. & Bahnemann, D. W. Environmental application of semiconductor photocatalysis. *Chem. Rev.* **95**, 69–96 (1995).
39. Herrmann, J. M. Heterogeneous photocatalysis: fundamentals and applications to the removal of various types of aqueous pollutants. *Catalysis Today* **53**, 115–129 (1999).

Author contributions

D.Z. and J.H.Y. synthesized semiconductor nanoparticles and analysed the hydrogel properties. S.B. assisted with the photocatalysis analysis. D.Z., J.H.Y., Q.S.W. and Q.G.W. designed the experiments, analysed the data and wrote the paper.

Additional information

Supplementary information accompanies this paper at http://www.nature.com/scientificreports

Competing financial interests: The authors declare no competing financial interests.

How to cite this article: Da Zhang, Yang, J., Bao, S., Wu, Q. & Wang, Q. Semiconductor nanoparticle-based hydrogels prepared via self-initiated polymerization under sunlight, even visible light. *Sci. Rep.* **3**, 1399; DOI:10.1038/srep01399 (2013).